Inorg. Chem. **1981**, *20*, 1051-1056

Contribution from University Chemical Laboratories,
Cambridge CB2 1EW, England

Structural and Ligand Field Parameters of Some Trigonally Distorted Tetrahedral Cobalt(II) and Nickel(II) Complexes

MALCOLM GERLOCH* and MARK R. MANNING

Received August 8, 1980

Single-crystal paramagnetic susceptibilities of the complexes $M(L_N^+)X_3$ (M = Co(II), Ni(II); X = Cl, Br; L_N^+ = *N*-ethyl-1,4-diazabicyclo[2.2.2]octonium) are reported throughout the temperature range 295–20 K. Unpolarized, crystal absorption spectra for both chloro complexes have been measured at 300 K and ca. 77 K. These spectra, together with those published for the bromo species, are analyzed within the angular overlap model to yield parameters which reflect a strong σ-donor capacity of the tertiary amine ligands, particularly in the nickel(II) complexes. The pattern of aom parameters correlates directly with coordination bond lengths throughout the series, both trends being rationalized in terms of the variable acceptor capacity of filled and half-filled orbitals within the d^8 and d^7 manifolds. Good estimates of the Racah *B* parameters have been obtained for the series of four complexes. The magnetic properties identify very low values of the spin–orbit coupling coefficients in the nickel complexes.

Introduction

Explicit recognition of the discrete functionality of individual ligands within the angular overlap model (aom) has revitalized ligand field theory as a probe of transition-metal bonding in complexes.[1,2] The interpretation of single-crystal paramagnetism and absorption spectra within sufficiently extensive term functional bases and without unnecessary idealizations of molecular geometry is proving increasingly successful in the characterization of separate σ- and π-bonding roles in metal–ligand interactions. In recent studies of several, formally tetrahedrally coordinated complexes of cobalt(II) and nickel(II), for example, we have demonstrated strong σ basicity[3] and strong π acidity[3,4] of coordinated triphenylphosphine groups and a moderate π-acceptor role for quinoline.[5] At the same time the donor capacities of halogens coordinated with these ligands have been shown to vary according to their relative number and in a manner reflecting the electroneutrality principle.

The present paper describes a study of the spectroscopy and paramagnetism of the relatively simple and geometrically ideal complexes $M(L_N^+)X_3$ in which M = Co(II) or Ni(II), X = Cl or Br, and L_N^+ is the tertiary amine, cationic ligand, *N*-ethyl-1,4-diazabicyclo[2.2.2]octonium (I). Garrett et al.[6] have reported single-crystal, polarized electronic absorption spectra of both bromo derivatives doped into the zinc analogues and interpreted their data as describing a C_{3v} distortion of tetrahedral coordination. We have recently completed X-ray structural studies[7] on all four complexes which confirm this geometry. We report here single-crystal, unpolarized absorption spectra for the pure $M(L_N^+)Cl_3$, M = Co(II) and Ni(II), systems at ca. 300 and ca. 77 K, together with complete crystal susceptibility determinations for all four complexes throughout the temperature range 20–300 K. All these data are analyzed within the angular overlap model for which we require the simple parameter set $e_\sigma(L_N^+)$, $e_\sigma(X)$, $e_\pi(X)$ for σ and π bonding to the tertiary amine and halogens. The study identifies a strongly basic tertiary amine, most particularly in the nickel(II) chromophores. The relative magnitudes of aom parameters of the cobalt and nickel complexes reflect dissimilarities in coordination bond lengths, and these are rationalized in terms of the differing acceptor properties of filled and half-filled orbitals within the d^8 and d^7 manifolds. The spin–orbit coupling coefficients determined from the present analysis of paramagnetic anisotropy of the nickel(II) species are very small, further[3] demonstrating a general trend throughout tetrahedrally coordinated nickel(II) complexes.

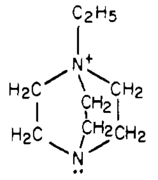

I

Table I. $Co(L_N^+)Br_3$: Interpolated, Experimental Principal and Average Crystal Susceptibilities (cgsu × 10^4 [a])

T/K	χ_a	χ_b	χ_c	$\bar{\chi}$	$\bar{\mu}/\mu_B$
295	94	92	88	91	4.64
275	100	98	94	97	4.63
255	107	105	101	104	4.61
235	116	114	109	113	4.61
215	125	123	118	122	4.58
195	137	135	129	134	4.57
175	152	149	142	148	4.55
155	171	166	159	165	4.53
135	196	189	180	188	4.51
115	230	220	209	220	4.49
95	277	264	249	263	4.47
75	352	334	313	333	4.47
55	477	449	414	447	4.43
35	741	678	610	676	4.35
20	1223	1090	929	1081	4.16

[a] 1 cgsu ≡ $4\pi \times 10^{-6}$ m^3 mol^{-1}.

Experimental Section

All four complexes $M(L_N^+)X_3$ (M = Co(II), Ni(II); X = Cl, Br) were prepared as described in the literature[8] and recrystallized from dimethylformamide at 80 °C under a slow stream of dry dinitrogen. Crystals selected for magnetic and spectroscopic measurements weighed from 0.8 to 7.0 mg. Those of both nickel compounds are very deliquescent but were successfully protected from the atmosphere by coating in Superglue, i.e., poly(methyl methacrylate). Such protection was unnecessary for the cobalt crystals which are only very

---

(1) M. Gerloch, *Prog. Inorg. Chem.*, **26**, 1 (1979).

(2) D. W. Smith, *Struct. Bonding (Berlin)*, **35**, 87 (1978).

(3) M. Gerloch and L. R. Hanton, *Inorg. Chem.*, preceding paper in this issue.

(4) J. E. Davies, M. Gerloch, and D. J. Phillips, *J. Chem. Soc., Dalton Trans.*, 1836 (1979).

(5) M. Gerloch and L. R. Hanton, *Inorg. Chem.*, **19**, 1692 (1980).

(6) B. B. Garrett, V. L. Goedken, and J. V. Quagliano, *J. Am. Chem. Soc.*, **92**, 489 (1970).

(7) M. R. Manning and P. R. Raithby, in preparation.

(8) J. V. Quagliano, A. K. Banerjee, V. L. Goedkin, and L. M. Vallarino, *J. Am. Chem. Soc.*, **92**, 482 (1970).

0020-1669/81/1320-1051$01.25/0

Table II. $Co(L_N^+)Cl_3$: Interpolated, Experimental Principal and Average Crystal Susceptibilities (cgsu × 10^4)

T/K	χ_1	χ_2	$\chi_3 \equiv \chi_b$	$\bar{\chi}$	$\bar{\mu}/\mu_B$
295	84	95	83	87	4.54
275	90	101	89	93	4.53
255	96	109	95	100	4.52
235	104	118	103	108	4.51
215	113	128	112	118	4.50
195	123	141	122	129	4.48
175	136	156	135	142	4.46
155	151	175	150	159	4.43
135	171	201	171	181	4.42
115	198	236	198	211	4.40
95	235	286	236	252	4.38
75	292	365	296	318	4.37
55	379	502	391	424	4.32
35	539	796	569	635	4.21
20	782	1332	866	993	3.99

Table III. $Ni(L_N^+)Br_3$: Interpolated, Experimental Principal and Average Crystal Susceptibilities (cgsu × 10^4)

T/K	χ_1	χ_2	$\chi_3 \equiv \chi_b$	$\bar{\chi}$	$\bar{\mu}/\mu_B$
295	48	59	57	55	3.59
275	51	64	61	59	3.59
255	55	69	66	63	3.59
235	59	75	71	68	3.58
215	63	82	77	74	3.57
195	68	90	84	81	3.55
175	75	101	93	90	3.54
155	82	114	104	100	3.52
135	92	130	117	113	3.49
115	104	153	135	131	3.47
95	121	188	160	156	3.45
75	144	239	198	194	3.41
55	176	321	257	251	3.32
35	234	499	374	352	3.14

slightly deliquescent. For the magnetic measurements, the procedure for the nickel crystals was to (i) dry with ethanol and acetone (twice), (ii) wrap in weighed aluminum foil, (iii) weigh, (iv) coat with Superglue, (v) orient on a Weissenberg goniometer with secondary protection by a gelatin capsule containing some molecular sieve, and (vi) measure susceptibilities in a dry helium atmosphere.

$Co(L_N^+)Br_3$ crystallizes with one molecule in the asymmetric unit in the orthorhombic space group *Pbca*. $Co(L_N^+)Cl_3$, $Ni(L_N^+)Cl_3$, and $Ni(L_N^+)Br_3$ crystallize in the monoclinic space group *Cc*, each with two closely similar molecules in the asymmetric unit.

Susceptibility Measurements. Susceptibilities were measured, using our single-crystal Faraday balance,[9] throughout the temperature range 20–300 K. For the orthorhombic $Co(L_N^+)Br_3$, crystals were oriented parallel to the symmetry axes *a*, *b*, and *c* yielding, on rotation of the magnet, $\chi_b\chi_c$, $\chi_a\chi_c$, and $\chi_a\chi_b$, respectively. Agreement of equivalent measurements of the different crystals oriented along these three different axes was better than 2%. Mean, interpolated, susceptibilities, corrected for a molar diamagnetism of $\chi_M^{dia} = -360 \times 10^{-6}$ cgsu, are listed in Table I. Susceptibility measurements for each monoclinic complex were made for crystals oriented parallel to *b*, *a* and *c*, yielding values for $\chi_1 < \chi_2$ in the *ac* plane, χ_b, $\chi_{c'}$, and χ_b, $\chi_{a'}$, respectively. Equivalent values of χ_b, determined for different crystals oriented parallel to *a* and *c*, agreed within 3% for $Co(L_N^+)Cl_3$ and $Ni(L_N^+)Br_3$ and within 6% for $Ni(L_N^+)Cl_3$. These errors derive from the problems of weighing these very deliquescent crystals before protective coating. Mean interpreted values of χ_1, χ_2, $\chi_3 \equiv \chi_b$ listed in Tables II–IV are corrected for molar diamagnetism by using $\chi_M^{dia} = -260 \times 10^{-6}$ cgsu for the chloro and -360×10^{-6} cgsu for the bromo complexes.

The orientation ϕ of χ_1 with respect to *a* (measured from the positive *a* vector through the positive *c* vector) is calculated to be +61° for $Co(L_N^+)Cl_3$ and −29° for $Ni(L_N^+)Br_3$, both values varying less than 1° throughout the temperature range. The value of ϕ for $Ni(L_N^+)Cl_3$ varies from +30° at 295 K to +7° at 20 K. As calculated ϕ values are especially sensitive to differences in measured principal χ values,

Table IV. $Ni(L_N^+)Cl_3$: Interpolated, Experimental Principal and Average Crystal Susceptibilities (cgsu × 10^4)

T/K	χ_1	χ_2	$\chi_3 \equiv \chi_b$	$\bar{\chi}$	$\bar{\mu}/\mu_B$
295	47	66	57	57	3.66
275	50	70	59	60	3.62
255	53	77	64	65	3.63
235	56	83	70	70	3.62
215	60	91	76	76	3.61
195	64	102	84	83	3.61
175	69	114	93	92	3.59
155	75	129	103	102	3.56
135	83	149	117	116	3.54
115	92	176	136	135	3.52
95	103	213	161	159	3.48
75	119	272	200	197	3.44
55	142	361	259	254	3.34
35	181	535	367	361	3.18
20	242	823	553	539	2.94

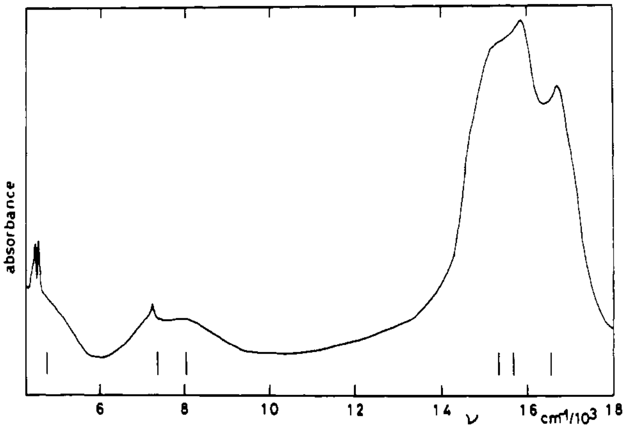

Figure 1. Unpolarized electronic spectrum of $Co(L_N^+)Cl_3$ at ca. 300 K.

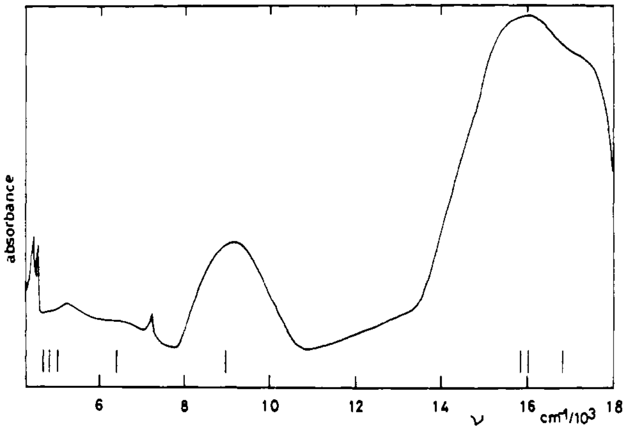

Figure 2. Unpolarized electronic spectrum of $Ni(L_N^+)Cl_3$ at ca. 300 K.

we must place little confidence in either the absolute values or the temperature dependence of these latter ϕ values in view of the considerable problems encountered with the measurement of very small (ca. 1 mg), very deliquescent crystals.

Spectra. Single-crystal, unpolarized absorption spectra for both chloro complexes were recorded with a Cary 17D spectrophotometer at ca. 300 K and with an Oxford Instruments continuous-flow CF100 cryostat at ca. 77 K. The spectra from 4000 cm^{-1} up to the charge-transfer adsorptions above 20 000 cm^{-1} are shown in Figures 1 and 2. The sharp features at ca. 4750 and 7250 cm^{-1} are also observed in the crystal adsorption of the zinc analogues and are therefore ascribed to vibrational rather than electronic d–d transitions. We also note that the spectra of solutions of the chloro complexes in nitromethane containing excesses of $(L_N^+)Cl^-$ are markedly different from those shown in Figure 2, implying that the chromophore co-

---

(9) D. A. Cruse and M. Gerloch, *J. Chem. Soc., Dalton Trans.*, 1613 (1977).

ordination integrity is not maintained in these solutions.

The Model

Calculations of energy levels and magnetic susceptibilities have been performed with the techniques and procedures[10,11] of the angular overlap model without restriction to the approximate C_{3v} symmetry of the chromophores. The model employed the complete maximum-spin bases $^3P + {}^3F$ for the nickel(II) and $^4P + {}^4F$ for the cobalt(II) complexes. Ligands were represented by placing their donor atoms exactly at their crystallographically determined[7] positions in the case of Co(L_N^+)Br_3. An averaging procedure was required for the other complexes in view of their having two molecules in the asymmetric unit. First we found that calculations of spectral and magnetic properties for the independent molecules in each cell differed by less than ca. 5% in general, though by ca. 10% in susceptibilities of the nickel complexes below ca. 60 K. The coordination geometries are closely similar within the unrelated pair in each case. For all three monoclinic systems, therefore, we have computed spectral and magnetic properties for the first molecule of the inequivalent pair: calculations of *crystal* susceptibilities have been made by appropriate tensorial addition of the susceptibilities of the reference molecule and of the reference molecule oriented as the second molecule of the inequivalent pair. In short, we have presumed that both orientations and magnitudes of principal molecular susceptibilities are identical for members of the inequivalent pairs of molecules in the asymmetric unit.

We have also presumed linear ligation of all ligands in the system, so leaving the aom parameter set $e_\sigma(L_N^+)$, $e_\pi(L_N^+)$, $e_\sigma(X)$, $e_\pi(X)$ for tertiary amine and halogens, respectively. All calculations were made, however, with $e_\pi(L_N^+) = 0$. In the approximate C_{3v} symmetry of these molecules, we obtain insufficient independent data with which to check the validity of this assumption. In each system, the parameter set was completed as usual with the Racah B parameter, spin–orbit ζ, and Stevens' orbital reduction factor k.

Fitting Spectra

We have found, no doubt as a result of the high approximate symmetry in these systems, that the magnetic susceptibilities do not provide clear definition of the aom or Racah B parameters. Our tactic throughout has been to use the spectra for this purpose, leaving the paramagnetism to establish ζ and k values.

Co(L_N^+)Br_3. Garrett et al.[6] have reported the room-temperature crystal adsorption spectrum of Co(L_N^+)Br_3 doped in the zinc analogue, band maxima associated with the $\rightarrow {}^4F$ bands occurring at 4420 and 7270 cm^{-1} and with those assigned as $\rightarrow {}^4P$ transitions being resolved at ca. 77 K at 14 620, 14 810, 14 990, 15 380, 15 700 and 16 100 cm^{-1}. Our initial tactic has been to determine values for the aom $e_\sigma(L_N^+)$, e_σ(Br), and e_π(Br) parameters which reproduce the positions of the two lower energy bands together with an overall spread of the components of ^4P of ca. 1500 cm^{-1}. Previous experience[5] and later checks allow estimation of the Racah B parameter by subsequent fitting of the absolute energy of the $\rightarrow {}^4P$ bands. The aom parameters were varied independently throughout the following ranges: $e_\sigma(L_N^+)$, 3000–6000 cm^{-1}; e_σ(Br), 3000–5000 cm^{-1}; e_π(Br) 0–2000 cm^{-1}. The gross splitting of the ^4P band is found to be especially sensitive to e_π(Br), values greater than 1000 cm^{-1} yielding unacceptably large separations of the ^4P components. The energy separation $^4T_1 \leftrightarrow {}^4T_2$ (T_d) is calculated too large for any parameter combination with $e_\sigma(L_N^+) > 4000$ cm^{-1}. Good reproduction of the observed spectral bands is found for the optimal parameter set: $e_\sigma(L_N^+)$, 4000 ± 200 cm^{-1}; e_σ(Br), 3500 ± 200 cm^{-1}; e_π(Br), 1000 ± 200 cm^{-1}. The quoted errors represent subjective estimates of ranges within which agreement between observed and calculated transition energies appears satisfactory. Optimal reproduction of the mean of transitions assigned to $\rightarrow {}^4P$ was achieved for this aom parameter set with $B = 700 \pm 10$ cm^{-1}. All calculations were performed at this stage with the spin–orbit parameter $\zeta = 500$ cm^{-1}, this value being chosen by experience[4,5] and hindsight. All choices of parameters within these aom, B, and ζ ranges yield a splitting pattern for components of the ^4P consisting of three slightly split doublets. We are quite unable to reproduce the relatively even splitting observed[6] experimentally, even when considering values for $e_\pi(L_N^+) \neq 0$. In view of the nonobservation of several spin-forbidden bands, we have not felt justified in performing full d^7 basis calculations in an attempt to rationalize the observed "^4P" splitting pattern in terms of the effects of, or combinations with, spin-doublet terms. Detailed comparison between observed and calculated eigenvalues within the complete spin-quartet manifold is presented in Table V.

Table V. Co(L_N^+)Br_3: Comparison between Observed Spectral Transition Energies (cm^{-1}) and Eigenvalues Calculated with Parameters Given in Table XI

calcd eigenvalues[a]		obsd[6] spectral peaks
15 817	$^4A_2$	16 100
14 973 14 638	^4E	15 700 15 380 14 990 14 810 14 620
7 653 6 926	^4E	7 270
4 914	$^4A_1$	4 420
3 871 3 513 3 171	$^4T_2$ (T_d)	
0	$^4A_2$	

[a] Averaged over spin quartets. Assignments (only) correspond to idealized C_{3v} symmetry.

Table VI. Co(L_N^+)Cl_3: Comparison between Observed Spectral Transition Energies (cm^{-1}) and Eigenvalues Calculated with Parameters Given in Table XI

calcd eigenvalues[a]		obsd spectral peaks
16 559	$^4A_2$	16 690
15 681 15 331	^4E	15 750 15 380
8 040 7 368	^4E	7 700
4 745	$^4A_1$	4 500
3 959 3 597 3 135	$^4T_2$ (T_d)	
0	$^4A_2$	

[a] Averaged over spin quartets. Assignments (only) correspond to idealized C_{3v} symmetry.

Co(L_N^+)Cl_3. The room-temperature, unpolarized crystal absorption spectrum of Co(L_N^+)Cl_3, shown in Figure 1, is characterized by peak maxima at 4500 and 7700 cm^{-1}, assigned to $\rightarrow {}^4F$ transitions, and 15 380, 15 750, and 16 690 cm^{-1}, assigned to components of $\rightarrow {}^4P$. A ca. 77 K the ^4P band sharpens slightly, having peak maxima of 15 380 (sh), 15 870, and 16 560 cm^{-1}; cf. Table VI. Little change is observed in the infrared spectrum on cooling. After exploration of a similar range of parameter space as for the bromo analogue and adoption of the same procedures, best fit parameters were virtually uniquely determined as $e_\sigma(L_N^+) = 4250 \pm 250$ cm^{-1}, $e_\sigma(Cl) = 3500 \pm 150$ cm^{-1}, $e_\pi(Cl) = 1100 \pm 200$ cm^{-1}, and

---

[10] M. Gerloch and R. F. McMeeking, *J. Chem. Soc., Dalton Trans.*, 2443 (1975).

[11] CAMMAG, a Fortran program by D. A. Cruse, J. E. Davies, J. H. Harding, M. Gerloch, D. J. Mackey, and R. F. McMeeking.

Table VII. $Ni(L_N^+)Br_3$: Comparison between Observed Spectral Transition Energies (cm^{-1}) and Eigenvalues Calculated with Parameters Given in Table XI and $\zeta = 120\ cm^{-1}$

calcd eigenvalues[a]		obsd[6] spectral peaks
16 251	$^3A_2$	16 200
15 569	^3E	16 100
15 046		15 200
		15 000
8 807	$^3A_2$	8 700
6 415	$^3A_1$	6 410
4 984	^3E	5 100
4 865		
4 525	$^3A_2$	
467	^3E	
0		

[a] Averaged over spin triplets. Assignments (only) correspond to idealized C_{3v} symmetry.

Table VIII. $Ni(L_N^+)Cl_3$: Comparison between Observed Spectral Transition Energies (cm^{-1}) and Eigenvalues Calculated with Parameters Given in Table XI and $\zeta = 125\ cm^{-1}$

calcd eigenvalues[a]		obsd spectral peaks
16 791	$^3A_2$	17 240
16 016	^3E	16 000
15 831		
8 962	$^3A_2$	9 090
6 393	$^3A_1$	6 410
4 981	^3E	5 260
4 809		
4 659	$^3A_2$	
268	^3E	
0		

[a] Averaged over spin triplets. Assignments (only) correspond to idealized C_{3v} symmetry.

$B = 740 \pm 10\ cm^{-1}$. Observed and calculated transition energies are compared in Table VI

$Ni(L_N^+)Br_3$. Spectral peaks in the crystal transmission spectrum at ca. 300 K for $Ni(L_N^+)Br_3$ have been reported[6] to lie at 5100, 6410, and 8700 cm^{-1}, assigned to $\rightarrow {}^3F$ transitions, and 15000, 15200, 16100, and 16200 cm^{-1} for $\rightarrow {}^3P$ transitions. The three lowest energy transitions together with the overall splitting of ca. 1200 cm^{-1} observed in the ^3P band provided rather exacting conditions for the determination of the aom parameters, optimal values being $e_\sigma(L_N^+) = 5900 \pm 150\ cm^{-1}$, $e_\sigma(Br) = 3000 \pm 150\ cm^{-1}$, and $e_\pi(Br) = 850 \pm 100\ cm^{-1}$. Subsequently a value $B = 720 \pm 10\ cm^{-1}$ was found to optimize reproduction of the mean $\rightarrow {}^3P$ transitions. Detailed comparison between observed and calculated transition energies is given in Table VII.

$Ni(L_N^+)Cl_3$. The room-temperature, unpolarized crystal absorption spectrum, shown in Figure 2, displays peak maxima at 5260, 6410, and 9090 cm^{-1}, assigned to components of $\rightarrow {}^3F$, and at 16000 with a shoulder at 17240 cm^{-1}, assigned to $\rightarrow {}^3P$. At ca. 77 K the two lowest energy bands are not noticeably more resolved. That at 9090 cm^{-1} sharpens a little on cooling, losing some contribution from the low-energy tail, presumably due to attenuation of "hot bands". The shoulder on the ^3P band at 17240 cm^{-1} is not observed on cooling to 77 K, and it appears that the intensity of this component of the ^3P transition increases relative to that of the main component at 16000 cm^{-1}. This behavior of intensities, though a small effect, is reminiscent of that found by Bertini et al.[12] for $Ni(PPh_3)X_3^-$ (X = Cl, Br) and has been ascribed to the approximate orbital doublet nature of the ground term.[3,12] Fitting all the bands observed in the room-temperature spectrum, as done for the other three complexes in this series, yielded the optimal parameter set $e_\sigma(L_N^+) = 6100 \pm 250\ cm^{-1}$, $e_\sigma(Cl) = 3250 \pm 100\ cm^{-1}$, $e_\pi(Cl) = 1000 \pm 200\ cm^{-1}$, $B = 760 \pm 10\ cm^{-1}$, and eigenvalues given in Table VIII.

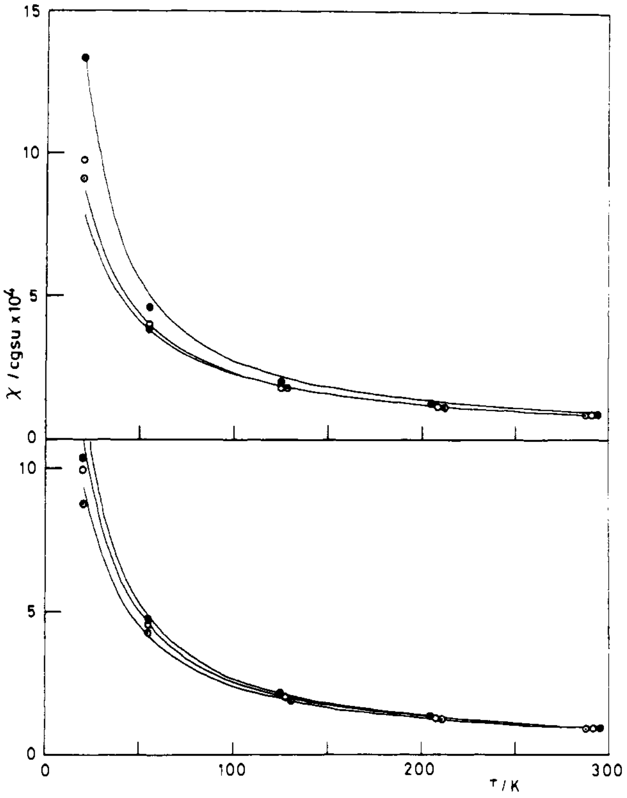

Figure 3. Comparison between observed principal crystal susceptibilities (continuous lines) with those calculated with parameter sets in Table XI for $Co(L_N^+)Cl_3$ (top) and $Co(L_N^+)Br_3$ (bottom).

Table IX

Orientation of Molecular Susceptibility Tensors at 125 K for $Co(L_N^+)X_3$ Complexes, Calculated with Parameter Sets of Table XI[a]

	$Co(L_N^+)Br_3$				$Co(L_N^+)Cl_3$		
	x	*y*	*z*		*x*	*y*	*z*
$K_1 = 177$	96.3	85.8	7.5	$K_1 = 157$	84.4	89.1	5.8
$K_2 = 209$	9.7	97.0	83.3	$K_2 = 192$	81.9	8.3	91.8
$K_3 = 213$	97.4	171.9	86.6	$K_3 = 199$	170.1	81.8	84.6

Reference Frames Defined with *z* Parallel to Co–N and with Respect to Orthogonalized Crystallographic Frames

	a	*b*	*c*	*a*	*b*	*c′*
x	0.3017	0.9177	0.2583	−0.9413	−0.3372	−0.0176[b]
y	−0.7724	0.0765	0.6305	−0.0063	−0.0347	0.9994
z	0.5589	−0.3897	0.7320	−0.3376	0.9408	0.0306

[a] Susceptibilities in cgsu × 10^3. [b] Direction cosines refer to "molecule 1" in the asymmetric unit.

Magnetic Susceptibilities

For all four complexes, optimal reproduction of the observed principal crystal paramagnetic susceptibilities was performed with use of the aom and Racah parameters determined from the spectra together with free variation of the spin–orbit and Stevens' orbital reduction factors, ζ and k.

Excellent fits, Figure 3, are obtained for both cobalt complexes for ζ in the range 450–550 cm^{-1} with k lying in the range 0.7–0.9 (bromo complex) or 0.6–0.7 (chloro): some degree of correlation between ζ and k values within these ranges is observed for best fit. The molecular susceptibility tensors, calculated with these optimal parameter sets are ap-

---

(12) I. Bertini, D. Gatteschi, and F. Mani, *Inorg. Chem.*, **11**, 2464 (1972).

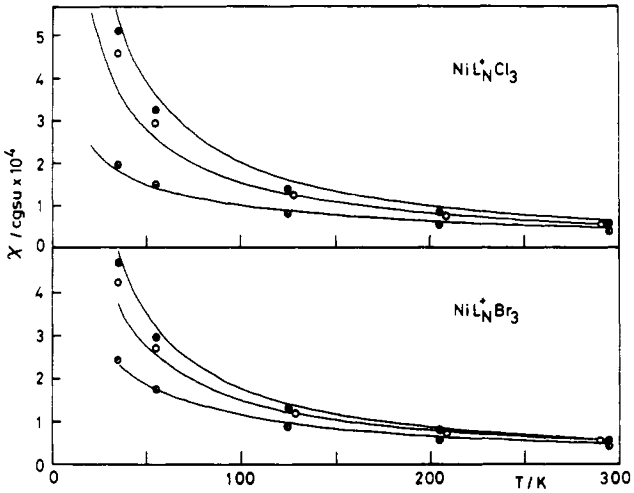

Figure 4. Comparison between observed principal crystal susceptibilities (continuous lines) with those calculated with parameter sets in Table XI for Ni(L_N^+)Cl_3 (top) and Ni(L_N^+)Br_3 (bottom).

proximately axial with the minimum principal susceptibilities lying nearly parallel to the Co–L_N^+ vectors: details at the representative temperature 125 K are shown in Table IX. For the chloro complex, the corresponding calculated value of the monoclinic ϕ angle is 61°, agreeing well with the value 61° determined by experiment.

Optimal fittings of the principal susceptibilities of the nickel complexes are obtained for ζ parameters which are fairly sharply defined with low values. For Ni(L_N^+)Br_3, we find $\zeta = 120 \pm 15$ cm^{-1} with $k = 0.75 \pm 0.10$, and for Ni(L_N^+)Cl_3, $\zeta = 130 \pm 20$ cm^{-1} and $k = 0.60 \pm 0.10$. Reproduction of the experimental susceptibilities of the bromo complex is good, less so for the chloro, as shown in Figure 4. Undoubtedly the experimental difficulities associated with the deliquescence of these crystals are partly responsible for the inexact agreement between theory and experiment; however, the necessity to base the model upon an assumed mean behavior of the two molecules in the crystallographically asymmetric unit represents an unfortunate limitation on the calculations. In the nickel systems, molecular magnetic anisotropies are greater, especially at low temperatures, so that trivial structural differences between the inequivalent molecules beget rather large anisotropy differences. The idealized averaging process performed here means, for example, that the maximum principal crystal susceptibility is calculated too high; further, the calculated monoclinic ϕ angle, a very sensitive function of molecular susceptibilities and orientation, is not in good agreement with experiment. However, the estimates of ζ should still be quite accurate, depending as it does more on the temperature variation of susceptibilities in these systems than on absolute values.

The calculated molecular susceptibility tensors are almost perfectly axial in both nickel complexes, with the maximum susceptibilities oriented closely parallel to the Ni–L_N^+ vectors, as shown at the representative temperature 125 K in Table X. The calculated monoclinic ϕ angles for bromo and chloro complexes are −28 and −30°, respectively, compared with the values deduced from experiment of −29°, and between +30° (at 295 K) and +7° (at 20 K).

Table X

Orientation of Molecular Susceptibility Tensors at 125 K for Ni(L_N^+)X_3 Complexes Calculated with Parameter Sets of Table XI[a]

	Ni(L_N^+)Br_3				Ni(L_N^+)Cl_3		
	x	y	z		x	y	z
$K_1 = 81$	119.2	150.6	85.9	$K_1 = 72$	42.4	47.7	92.1
$K_2 = 82$	29.2	119.2	90.0	$K_2 = 72$	132.3	42.3	88.0
$K_3 = 184$	88.1	86.5	4.1	$K_3 = 203$	92.9	89.9	177.2

Reference Frames Defined with z Parallel to Ni–N and with Respect to Orthogonalized Crystallographic Frames

	a	b	c'	a	b	c'
x	−0.9169	−0.1257	0.3787[b]	−0.9413	−0.3372	−0.0176[b]
y	−0.1509	0.9878	−0.0375	−0.0063	−0.0347	0.9994
z	−0.3694	−0.0916	−0.9248	−0.3376	0.9408	0.0306

[a] Susceptibilities in cgsu × 10^3. [b] Direction cosines refer to "molecule 1" in the asymmetric unit.

Table XI. Summary of Parameter Values Optimally Reproducing Observed Spectra and Paramagnetism[a]

complex	$e_\sigma(L_N^+)$	e_σ(X)	e_π(X)	B	ζ	k
Co(L_N^+)Cl_3	4250	3500	1100	740	500	0.7
Co(L_N^+)Br_3	4000	3500	1000	700	500	0.8
Ni(L_N^+)Cl_3	6100	3250	1000	760	130	0.6
Ni(L_N^+)Br_3	5900	3000	850	720	120	0.8

[a] Energies in cm^{-1} [$e_\pi(L_N^+) = 0$ by assumption].

Table XII. Comparison of Coordination Bond Lengths (Å) in M(L_N^+)X_3 Species[7]

bond	Co(L_N^+)-Br_3	Co(L_N^+)Cl_3[a]		Ni(L_N^+)Br_3[a]		Ni(L_N^+)Cl_3[a]	
M-N	2.13	2.08	2.10	2.03	2.04	2.04	2.04
M-X	2.40	2.26	2.21	2.38	2.38	2.22	2.22
	2.37	2.25	2.27	2.40	2.38	2.26	2.24
	2.37	2.27	2.28	2.34	2.37	2.25	2.26
mean M-N	2.13	2.09		2.09		2.04	
mean M-X	2.38	2.26		2.38		2.24	

[a] Two molecules in the asymmetric unit.

Discussion

In Table XI we collect the parameter sets which best reproduce the observed spectra and magnetism of these four complexes. Striking consistencies and trends are illustrated in the ligand field aom parameters, in B values, and in spin–orbit coupling coefficients. Throughout, the σ basicity of the tertiary amine is larger than that of the halogens, markedly so for the nickel complexes. Qualitatively this occasions no surprise, nor does the observation that all aom parameters are somewhat greater for the chlorine than for the bromine ligands. Similarly the larger B values for the chloro complexes compared with the bromo are in line with the nephelauxetic series.[13,14] However, the magnitude of the increase in $e_\sigma(L_N^+)$ values on replacing cobalt with nickel does not appear immediately sensible. Further if the increase is ascribed to an increase in the effective nuclear charge on the central metal, we might inquire why there are no corresponding increases—in fact, somewhat the opposite—in the aom parameter values for the halogens.

Before attempting the answer this question, however, it is rewarding to review the aom parameters in comparison with bond lengths in the coordination shells of this series of complexes (Table XII). We note that the mean metal–halogen bond lengths do not vary significantly with metal whereas the metal–amine distances are significantly shorter in the nickel complexes. The aom parameters in Table XI are thus a direct reflection of the pattern of bond lengths summarized in Table XII, and it is encouraging to observe these trends independently demonstrated by the spectroscopic and structural techniques.

---

(13) C. K. Jørgensen, "Modern Aspects of Ligand Field Theory", North Holland Publishing Co., Amsterdam, 1971.

(14) M. Gerloch and R. C. Slade, "Ligand Field Parameters", Cambridge University Press, London, 1973.

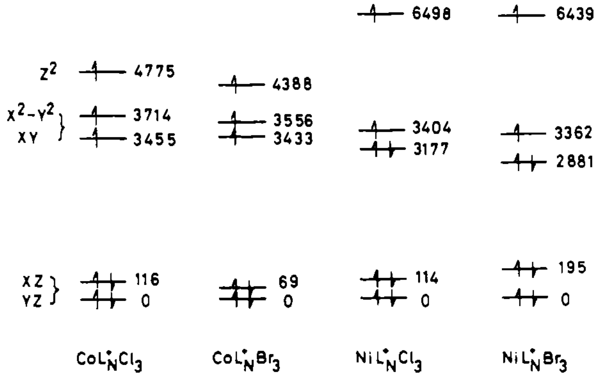

Figure 5. Orbital energies corresponding to parameter sets in Table XI, but with $\zeta = 0$. Labels describe predominant orbital parentages.

As we expect to observe, *on average*, a higher position in the spectrochemical series and shorter coordination bond lengths for the nickel complexes, we view the pattern of aom parameters and bond lengths as describing a situation in which the nickel–halogen interactions are relatively weak, compensated by a significantly increased nickel–amine bond strength. This bonding picture may be rationalized directly in a manner analogous to that recently proposed[15] within a series of seven-coordinate complexes. In Figure 5 we show *orbital* energy diagrams corresponding to the best fit parameters of Table XI, except, for simplicity, that we take $\zeta = 0$. The labeling represents dominant orbital parentage, though in the high pseudosymmetry of these complexes, the orbitals are between 80 and 100% "pure". On passing from the d^7, cobalt(II), systems to the d^8, nickel(II), the extra electron is housed in $d_{x^2-y^2}/d_{xy}$ orbital pair. Accordingly, the overall acceptor properties of this orbital pair are less for nickel(II) than for cobalt(II). These orbitals interact exclusively with the halogen ligands because (a) they are somewhat directed toward them and (b) the tertiary amine ligand is not considered to have any δ-bonding function toward the metal. Consequently, the donor halogens should be less well bound in the nickel complexes. The general operation of the electroneutrality principle then requires a greater electron donation from the amine ligand. The effect on the nickel–amine bond length and spectroscopic parameters is especially dramatic, presumably, by virtue of the extra effective nuclear charge of the nickel atom together with there being only one amine ligand in the chromophore available to donate the required charge.

This description of the detailed bond lengths and ligand field parameters in this series emphasizes again that bonding is a "mutal affair" and that the donor capacity of a ligand depends upon the acceptor capacity of the remaining ligated metal moiety. While all this is well understood throughout general chemistry, it is only relatively recently that some direct measure of the electron distribution in complexes has been available through ligand field techniques.

The interelectron repulsion B parameters in Table XI reveal a consistently greater nephelauxetic effect for bromine ligands than for chlorine. Typically the gross reduction of B values from the corresponding free ion values[16] is similar for nickel(II) and for cobalt(II)—$B_0(\mathrm{Co}^{2+}) = 1115$, $B_0(\mathrm{Ni}^{2+}) = 1084$ cm^{-1}. We presume that the formation of these complexes together with the operation of the electroneutrality principle leaves essentially similar electron density distributions close to the metal nuclei.

The spin–orbit coupling parameters in these complexes contribute to the trend recently discussed[3] in which "tetrahedral" nickel(II) systems appear characterized by very low spin–orbit coefficients. Two mechanisms for this have been proposed.[3] That of Collingwood et al.[17] centers upon the sign of an expansion coefficient in the molecular orbitals of the $^3T_1$ term such that contributions to ζ from the ligands tend to cancel that of the central metal: this argument seems especially persuasive for $\mathrm{NiI_4}^{2-}$ ions where the large ζ value of the iodine ligands appears to have led to the observed value for the complex, $\zeta \approx 15$ cm^{-1}. The alternative proposal[3] is that all tetrahedrally coordinated nickel(II) complexes are subject to the Ham effect[18] to some extent. This seems especially appropriate for the present complexes in view of the relatively small spin–orbit coefficients of the bromine and especially of the chlorine ligands; and also by virtue of the essentially orbital doublet nature of the ground terms in these pseudo-C_{3v} systems. While it does not appear possible at this stage to quantify the separate roles of these two proposed mechanisms for the reduction in ζ values, a more detailed comparison being given in ref 3, low ζ values in tetrahedral d^8 systems appear established as an empirical norm.

Acknowledgment. We thank the Science Research Council for a Research Studentship (to M.R.M). We are grateful to Rank Xerox for the loan of the Cary 17D spectrophotometer.

Registry No. $\mathrm{Co(L_N{}^+)Cl_3}$, 76334-18-4; $\mathrm{Co(L_N{}^+)Br_3}$, 26721-62-0; $\mathrm{Ni(L_N{}^+)Cl_3}$, 76334-19-5; $\mathrm{Ni(L_N{}^+)Br_3}$, 26721-63-1.

---

(15) M. Gerloch and I. Morgenstern-Baderau, *Inorg. Chem.*, **18**, 3225 (1979).

(16) J. S. Griffith, "Theory of Transition Metal Ions", Cambridge University Press, London, 1961.

(17) J. E. Collingwood, P. Day, and R. G. Denning, *J. Chem. Soc., Faraday Trans. 2*, **69**, 591 (1973).

(18) F. S. Ham, *Phys. Rev.* [*Sect.*] *A*, **138**, 1727 (1965).